Study of Perovskite $CsPbBr_3$ Detector Polarization and its mitigation with Ultra-high X-ray Flux

Lei Pan[1], Indra Pandey[1,2], Zhifu Liu[3], John A. Peters[3,4], Duck Young Chung[2], Conny Hansson[5], Bruce W. Wessels[3], Antonino Miceli[6], and Mercouri G. Kanatzidis[1,2,3]*

[1]*Department of Chemistry, Northwestern University, Evanston, IL 60208, USA*
[2]*Materials Science Division, Argonne National Laboratory, Lemont, IL 60439, USA*
[3]*Department of Materials Science and Engineering, Northwestern University, Evanston, IL 60208, USA*
[4]*Department of Chemistry, Physics, & Engineering Studies, Chicago State University, Chicago, IL 60608*
[5]*SLAC National Accelerator Laboratory, Menlo Park, CA 94025*
[6]*X-ray Science Division, Argonne National Laboratory, Lemont, IL 60439, USA*

*Correspondence to: m-kanatzidis@northwestern.edu

Abstract

High-flux capable semiconductor X-ray detectors are essential in various applications, but the detrimental effects of detector polarization limit their use in many cases. Here, we studied the polarization of perovskite $CsPbBr_3$ semiconductor detectors using ultra-high flux synchrotron X-rays (10^6 – 10^{12} photons s^{-1} mm^{-2} at 58.61 keV). The $CsPbBr_3$ detectors did not show immediate polarization prominently until a flux higher than 10^{10} photons s^{-1} mm^{-2}. Using the pump-and-probe technique, we visualized the spatial and temporal effects of polarization. The polarized region, represented by reduced photocurrent, extended beyond the area under direct irradiation, and the reduced photocurrent persisted after potential de-polarization treatments, such as reversing bias voltage. We found that stronger applied electric fields and fewer carrier traps can mitigate polarization, represented by less photocurrent deficit. By examining the detectors' current response under controlled ambient light, low and high flux X-ray, we studied the trap filling and release behavior of $CsPbBr_3$. We discovered that the polarization is caused by partial detector damage due to deep defects generated by the ultra-high flux X-ray irradiation. Our work provides insight into $CsPbBr_3$ polarization under extremely intense X-ray radiation and shows that reducing crystal defects and increasing detector bias voltage are effective solutions.

Introduction

Room temperature high Z semiconductor detectors are widely used for hard radiation detection in various fields such as medical imaging, nuclear security, and scientific research[1-5]. These applications often require high photon flux, for example, ~10^9 photons s^{-1} mm^{-2} (shortened as p s^{-1} mm^{-2}) in medical Computed Tomography scans[6]. However, detector polarization remains a major issue that limits and degrades semiconductor detector performance. Detector polarization occurs when excessive space charge buildup inside the semiconductor distorts the electric field profile. The polarization can be classified as radiation-induced and bias-induced, depending on the origin of the space charge buildup. Radiation-induced polarization is caused by charge carrier trapping at deep defects and becomes more prominent at high flux levels. A theoretical model has been developed to explain the process of radiation-induced polarization and its contributing factors[7]. Briefly, radiation-induced polarization is due to charge carrier trapping at deep defects and becomes progressively prominent at high flux level. Both CdTe and CdZnTe (CZT) were reported to suffer from radiation-induced polarization. A CdTe detector showed significant polarization at an X-ray flux of ~ 9×10^{10} keV/s/mm^2 [8]. A CZT detector was reported to polarize at flux of 10^6 p s^{-1} mm^{-2} and became significantly polarized when flux increased to 10^9 p s^{-1} mm^{-2} [6]. The recently developed "high-flux" CZT was reported to show good photocurrent linearity in flux range of 10^7 – 10^{10} p s^{-1} mm^{-2} [9]. On the other hand, the bias-induced polarization can be caused by ion migration or deep defect levels. TlBr detectors were reported to suffer from significant ion migration issues[10,11]. Bias-induced polarization in a CdTe Schottky detector was attributed to the ionization of deep defect levels under the influence of applied electric fields[12]. Various methods have been reported to mitigate polarization, including switching the bias polarity for TlBr detector[13,14], and infrared illumination for CZT detector[15].

Perovskites have recently emerged with promising performance as semiconductor radiation detectors[16]. While thin/thick films can have large area and flexibility desired as flat panel X-ray imager[17], bulk single crystals are more favored in applications where high detection efficiency and spectroscopic resolution capability are a priority. Among different types of perovskites, the all-inorganic perovskite $CsPbBr_3$ has demonstrated excellent performance for gamma ray spectroscopy[18,19], X-ray photon counting[2], and X-ray detection in energy integrating mode[20]. The $CsPbBr_3$ detector from melt growth in our previous work can be operated stably for over 120 hours

under low flux gamma ray source (^{57}Co with activity ~ 200 μCi) without apparent bias-induced polarization[19], which indicates that ion migration is not a concern in spectrometer grade $CsPbBr_3$. However, we previously further showed that $CsPbBr_3$ detector exhibited radiation-induced polarization under X-rays with high flux (~10^5 p s^{-1} mm^{-2}) for several hours irradiation [2], or with ultra-high flux (10^{11} - 10^{12} p s^{-1} mm^{-2}) for several seconds irradiation[5]. The performance of $CsPbBr_3$ detectors under high and ultra-high X-ray flux conditions is of practical importance, which, however, has not been fully understood. Research in this area is crucial to determine the capabilities and limitations of $CsPbBr_3$ detectors in real-world applications where high flux radiation is present, such as medical imaging and scientific research[1,4,21]. Under high flux, such as 10^7 – 10^9 p s^{-1} mm^{-2} commonly used in medical imaging, the time for stable operation without prominent polarization should be much longer than typical usage time scales. Moreover, the ability to sustain ultra-high photon fluxes (higher than 10^{10} p s^{-1} mm^{-2}) without immediate polarization could enable $CsPbBr_3$ to play a critical role in synchrotron X-ray based techniques[22-24]. Understanding the behavior of $CsPbBr_3$ detector under high and ultra-high flux is essential for designing and developing detectors that can effectively operate under these conditions.

In this work, we investigated $CsPbBr_3$ single crystal semiconductor detector polarization with a wide range and ultra-high flux (10^6 - 10^{12} p s^{-1} mm^{-2} with energy 58.61 keV) provided by a synchrotron X-ray beamline. Schottky $CsPbBr_3$ detectors with Bismuth(Bi)/$CsPbBr_3$/Bi and Au/$CsPbBr_3$/Bi configurations were tested. A guard ring electrode was used to reduce leakage current, increase bias voltage and improve detector current stability. The pump-and-probe technique was used to observe the spatial extent and temporal evolution of the polarization. We found that a stronger applied electric field can effectively mitigate polarization. $CsPbBr_3$ crystals of differing quality (i.e., number of defects) were compared and the crystal with more defects showed more severe polarization. We further studied the $CsPbBr_3$ trap filling and release behavior by examination of the detector current response under controlled ambient light, and low and high flux X-rays. The study found that $CsPbBr_3$ detector polarization under ultra-high flux (e.g., >10^{10} p s^{-1} mm^{-2}) was not healed by conventional post-polarization treatments such as reversing bias direction or light illumination, which suggests a detector damage caused by the ultra-high flux X-ray irradiation. It is noteworthy that only partial detector damage occurred because the photocurrent of the polarized region did not reduce to zero. The thermally stimulated current measurements indicate that the polarized region is not electrically active at temperatures between

79 K and 315 K, suggesting the formation of deep defect levels that are responsible for the partial detector damage. This highlights the need for further research and development of methods to mitigate polarization in $CsPbBr_3$ detectors under ultra-high flux conditions by reducing the number of deep defect levels.

Results and Discussion

$CsPbBr_3$ detectors and experimental setup

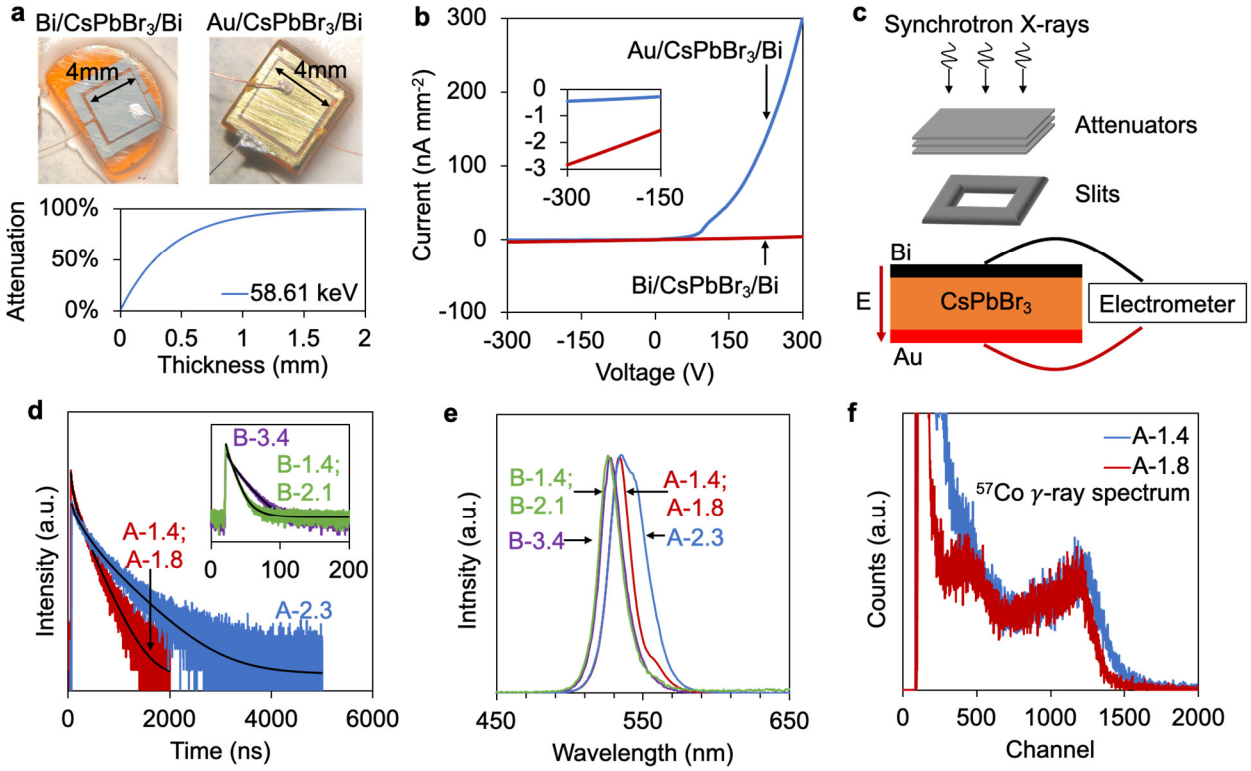

Fig 1. $CsPbBr_3$ detectors and experimental setup. a, $CsPbBr_3$ detector structures and attenuation of 58.61 keV X-ray by $CsPbBr_3$. Center electrode area is 4×4 mm^2. **b,** dark I-V curve of the Bi/$CsPbBr_3$/Bi and the Au/$CsPbBr_3$/Bi detector structure. **c,** experimental setup for detector testing under synchrotron X-ray. **d, e,** Time-resolved photoluminescence decay time and steady state photoluminescence emission spectra of different $CsPbBr_3$ crystals. The decay time was measured at peak emission wavelength. A FS5 spectrofluorometer (Edinburgh Instruments) was used for photoluminescence measurements. The crystals A-1.4 and A-1.8 were taken from the same part of a ingot. The crystals B-1.4 and B-2.1 were from the same part of a ingot. **f,** ^{57}Co gamma ray energy spectrum of device A-1.8 and A-1.4. A preamplifier (eV-550), a shaping amplifier (ORTEC 572A), and a multi-channel analyzer (ORTEC 927) were used for gamma spectrum acquisition.

Table 1. Dimensions and structures of $CsPbBr_3$ detectors.

	Bi/$CsPbBr_3$/Bi	Au/$CsPbBr_3$/Bi					
Thickness (mm)	1.8	1.4	1.8	2.3	1.4	2.1	3.4
PL decay time (ns)	50	110	110	501	5	5	11
Guard ring electrode	No	Yes	Yes	Yes	Yes	Yes	Yes

We fabricated Schottky type $CsPbBr_3$ detectors with Bi/$CsPbBr_3$/Bi and Au/$CsPbBr_3$/Bi structure (**Fig 1a**) where the $CsPbBr_3$ crystals were grown from Bridgman method described in detail in our previous work [19]. The dimensions of the $CsPbBr_3$ detectors tested in this work are listed in **Table 1**. According to our previous work[20,25], Bi forms Schottky contact with p-type $CsPbBr_3$ single crystal with a Schottky barrier ~ 1 eV, while Au forms Ohmic contact with $CsPbBr_3$. The Bi/$CsPbBr_3$/Bi detector structure has Schottky contact on both sides so that a small leakage current can be obtained regardless of the bias voltage direction (**Fig 1b**)[25]. In comparison, the Au/$CsPbBr_3$/Bi detector structure has small leakage current at the reverse bias voltage direction that is defined as the electric field direction from Bi pointing to Au, and large leakage current at forward bias voltage direction (**Fig 1b**). The 1/e absorption depth of $CsPbBr_3$ for 58.61 keV photon provided by the synchrotron beamline is 0.41 mm. Hence, $CsPbBr_3$ (density 4.75 g cm^{-3}) can attenuate ~ 91% and ~ 99% of the 58.61 keV X-ray photons with 1 mm and 2 mm thickness, respectively (**Fig 1a**). Given the limited penetration depth of the 58.61 keV X-rays, when the Bi anode is irradiated, holes contribute more to the total induced signal according to the Shockley-Ramo theorem[26], which may be called "hole collection mode". Similarly, irradiating the Bi side of the detector and biasing it as a cathode may be called "electron collection mode". We tested the $CsPbBr_3$ detectors in hole collection mode, unless specifically noted otherwise, as there is a lower tendency for hole trapping compared to electron trapping (mobility lifetime product of holes and electrons for $CsPbBr_3$ is $\mu_h\tau_h = 1.34\times10^{-3}$ cm^{-2} V^{-1} and $\mu_e\tau_e = 8.77\times10^{-4}$ cm^{-2} V^{-1}, respectively [19]). The $CsPbBr_3$ detectors worked at current mode with voltage applied and current measured by an electrometer (Keithley 6517B). The synchrotron X-ray flux was changed by changing the number of attenuators and the X-ray beam area was controlled by adjustable slits (**Fig 1c**).

In our previous work, we developed an efficient method using photoluminescence (PL) spectroscopy to screen for $CsPbBr_3$ crystal quality, specifically nonradiative defects[5]. Typically, the longer the PL decay time, the fewer non-radiative recombination defects present in the perovskite[27,28]. Here, we selected six $CsPbBr_3$ crystals, three with significantly longer PL decay

time than the rest (**Fig 1d**). Quantitatively, the PL decay time is characterized by the intensity averaged decay time τ_{ave}. The experimental PL decay data is fitted to a multi-exponential decay equation, $I(t) = A_1 e^{-t/\tau_1} + A_2 e^{-t/\tau_2} + A_3 e^{-t/\tau_3}$, where $I(t)$ is PL intensity, A_1, A_2, A_3 are proportionality coefficients. The τ_{ave} is calculated as $\tau_{ave} = \sum A_i \tau_i^2 / \sum A_i \tau_i$. The τ_{ave} of the six $CsPbBr_3$ crystals are listed in **Table 1**. Additionally, $CsPbBr_3$ crystals with long τ_{ave} typically have longer emission wavelength (**Fig 1e**), which is consistent with our previous report[5]. For convenience, we arbitrarily classify the $CsPbBr_3$ crystals with long τ_{ave} (e.g., $\tau_{ave} > 60$ ns) as grade A crystal, while the $CsPbBr_3$ crystals with $\tau_{ave} < 40$ ns as grade B crystal. Hence, to distinguish the six crystals, we name them in format of "grade-thickness", so that the 6 crystals are named as A-1.4, A-1.8, A-2.3, B-1.4, B-2.1, B-3.4. The fewer number of nonradiative defects represented by the long τ_{ave} also manifest as gamma ray spectroscopy capability. Devices made of $CsPbBr_3$ crystals with long τ_{ave} usually can resolve the ^{57}Co gamma ray photopeak. As shown in **Fig 1f,** device made of crystal A-1.4, A-1.8 could resolve the 122 keV photopeak, while the devices made of B-1.4, B-2.1, B-3.4 had significantly lower pulse amplitude and could not resolve the 122 keV photopeak.

Spatial and temporal evolution of $CsPbBr_3$ polarization

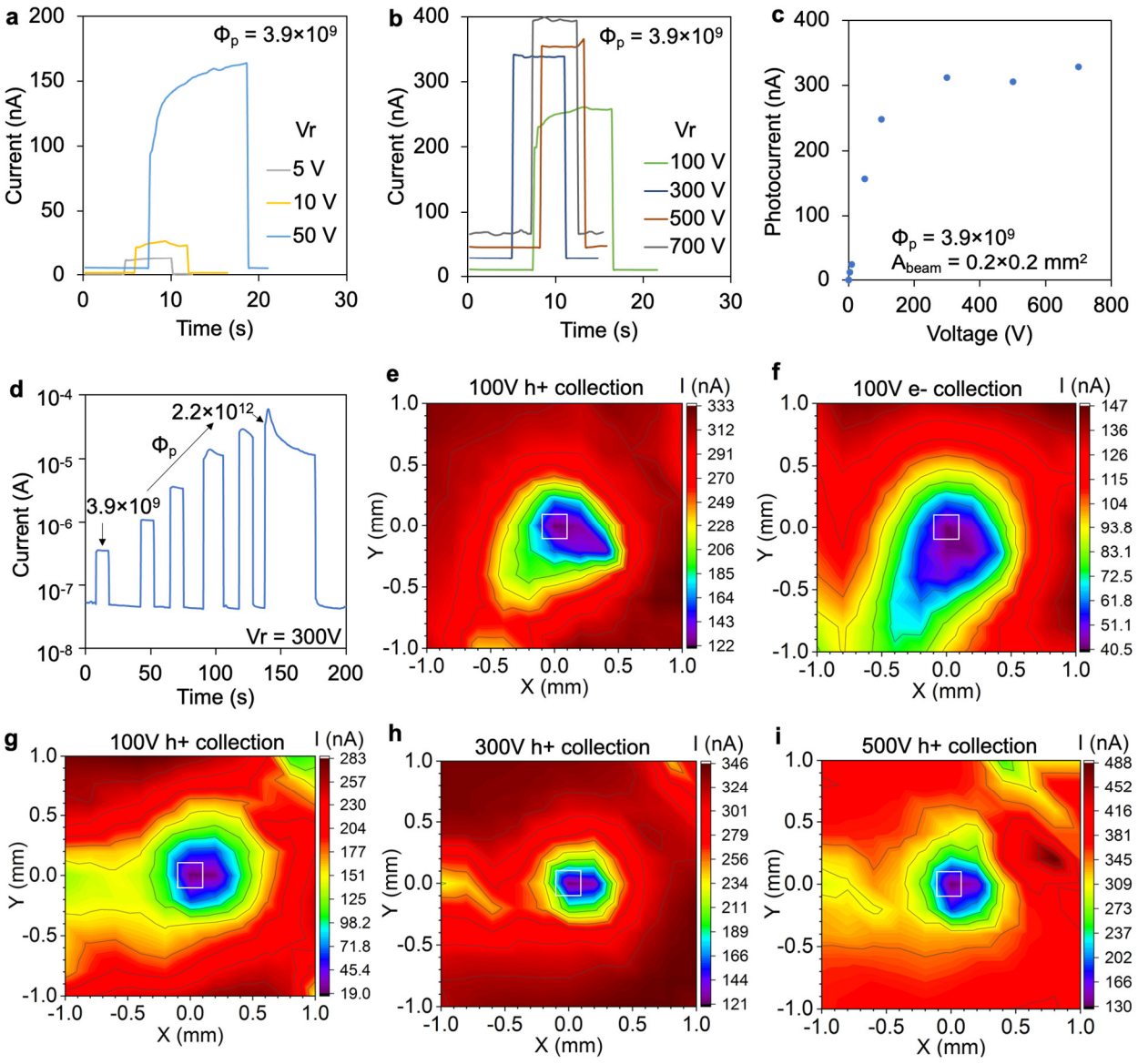

Fig 2. Study of $CsPbBr_3$ detector polarization with pump-and-probe by synchrotron X-ray. The Bi/$CsPbBr_3$/Bi detector was used for testing. **b,** Bi/$CsPbBr_3$/Bi current response to X-ray flux fixed at $\Phi_p = 3.9\times10^9$ p s^{-1} mm^{-2} at different bias voltage Vr (beam size $A_{beam} = 0.2\times0.2$ mm^2). **c,** photocurrent as a function of bias voltage calculated from data shown in **b**. **d**, Bi/$CsPbBr_3$/Bi current response to X-ray flux in the range $\Phi_p = 3.9\times10^9$ p s^{-1} mm^{-2} to $\Phi_p = 2.2\times10^{12}$ p s^{-1} mm^{-2} (Vr = 300 V, beam size $A_{beam} = 0.2\times0.2$ mm^2). **e, f, g, h, i,** photocurrent probed by $\Phi_p = 3.9\times10^9$ p s^{-1} mm^{-2} after pump at $\Phi_p = 2.2\times10^{12}$ p s^{-1} mm^{-2} where prominent polarization was induced. Beam size $A_{beam} = 0.2\times0.2$ mm^2. **e, f,** the h+ and e- collection means hole and electron collection mode, respectively, for a same polarized spot. **g, h, i,** photocurrent measured at different bias voltage for a same polarized spot.

Since bias voltage can affect polarization[6,7], we first tested the current response of the Bi/$CsPbBr_3$/Bi detector to a fixed X-ray flux of $\Phi_p = 3.9\times10^9$ p s^{-1} mm^{-2} at different bias voltage

Vr . First, we applied a bias voltage to the $CsPbBr_3$ detector, and the dark current was continuously measured. Then the X-ray beam was turned on and off manually by controlling the shutter. As depicted in **Fig 2a** and **Fig 2b**, increasing the bias voltage resulted in an increase in the signal current of the $CsPbBr_3$ detector, accompanied by a decrease in the rise time of the current. For instance, the rise time longer than 10 seconds at 50 V was significantly reduced to shorter than 1 second when the bias voltage was increased to 500 V. The prolonged rise time of the current observed at low bias voltage (e.g., longer than 10 seconds at 50 V) can be attributed to the filling of traps by free charge carriers generated by X-rays. As more traps are filled, a higher number of carriers can be extracted, resulting in an increased signal current. This extended rise time is a manifestation of radiation-induced polarization. On the other hand, increasing the bias voltage significantly shortened the rise time (e.g., shorter than 1 second at 500 V), indicating that a higher bias voltage can reduce charge trapping and, consequently, decrease polarization. However, the detector current could become unstable if the bias voltage is overly high. The dark current and signal current at 700 V showed fluctuation compared to 300 V (**Fig 2b**). **Fig 2c** shows the photocurrent (difference between signal current with X-ray "on" and dark current) as a function of bias voltage calculated from data in **Fig 2b**. The photocurrent increases as bias voltage increases and approaches saturation as charge collection efficiency approach ~100% at higher bias voltage, which means polarization is not affecting charge carrier collection at flux $\Phi_p = 3.9\times10^9$ p s^{-1} mm^{-2} when bias voltage higher than 100 V (56 V mm^{-1}). Compared to the stable signal current at 3.9×10^9 p s^{-1} mm^{-2}, the current started to become unstable above 3.9×10^9 p s^{-1} mm^{-2} (**Fig 2d**). The signal current showed a quick increase and then decay behavior. As the traps are being filled in, more charge carriers contribute to the slowly increasing signal current. As the space charge density continues to increase due to charge trapping, the electric field inside the detector starts to collapse, which leads to the current decay. The current decay at $\Phi_p = 2.2\times10^{12}$ p s^{-1} mm^{-2} was prominent (**Fig 1d**), which indicates significant radiation-induced polarization.

To study the spatial and temporal evolution of the $CsPbBr_3$ polarization, we intentionally induced polarization by irradiating a specific region of the detector with flux 2.2×10^{12} p s^{-1} mm^{-2} for 1 min ("pump" process), and then performed a raster scan of the current signal with a lower flux 3.9×10^9 p s^{-1} mm^{-2} since polarization at this level is negligible ("probe" process). The X-ray beam size was $A_{beam} = 0.2\times0.2$ mm^2. The raster scan area was 2×2 mm^2 with step size 0.2 mm and a dwell time of 10 s at each step. The directly irradiated area was located at the center of the scan area (marked

by the square). We first compared the photocurrent of a same polarized spot (noted as Spot 1) in hole and electron collection mode (**Fig 2e** and **Fig 2f**). The same region of the detector was irradiated, while the bias voltage polarity was reversed for respective hole and electron collection. The region affected by polarization was larger than the directly irradiated area of 0.2×0.2 mm^2, which might be due to lateral diffusion and trapping of the X-ray generated free carriers. The photocurrent in hole collection mode is much higher than that in the electron collection mode for both the polarized and non-polarized areas, which is consistent with less hole trapping in these crystals. It is noteworthy that the photocurrent in the polarized region does not fall to zero, indicating that complete damage from the ultra-high flux X-ray is probably not the case.

We further compared the effect of bias voltage on $CsPbBr_3$ polarization. The photocurrent of a same polarized spot (noted as Spot 2) in hole collection mode was measured at 100 V, 300 V, and 500 V (**Fig 2g** and **Fig 2h, Fig 2i**). As the bias voltage increased from 100 V to 300 V, the photocurrent increased for both the polarized and non-polarized areas. Most non-polarized area has photocurrent in the range of ~ 345 nA to 381 nA at 500 V (**Fig 2i**), slightly higher than the range of ~ 324 nA to 346 nA at 300 V (**Fig 2h**).In addition, the photocurrent of the directly irradiated area increased from 121 nA at 300 V to 130 nA at 500 V, which shows that high bias voltage could mitigate the polarization. However, increasing the bias voltage could cause signal current instability. As shown in **Fig 2i** at 500 V, a localized non-polarized area (near the right center of the figure) produced a photocurrent in the range of ~ 381 - 488 nA that is higher than the other non-polarized area mentioned above with photocurrent in the range ~ 345 nA - 381 nA. Such photocurrent local bump is due to current temporal fluctuation caused by the overly high bias voltage. The scans at 100 V, 300 V, and 500 V were performed consecutively, with each scan lasting for ~ 17 mins. After these three scans which were completed in ~1 hour, the detector did not recover from the polarization under the testing conditions.

Influence of crystal quality on polarization

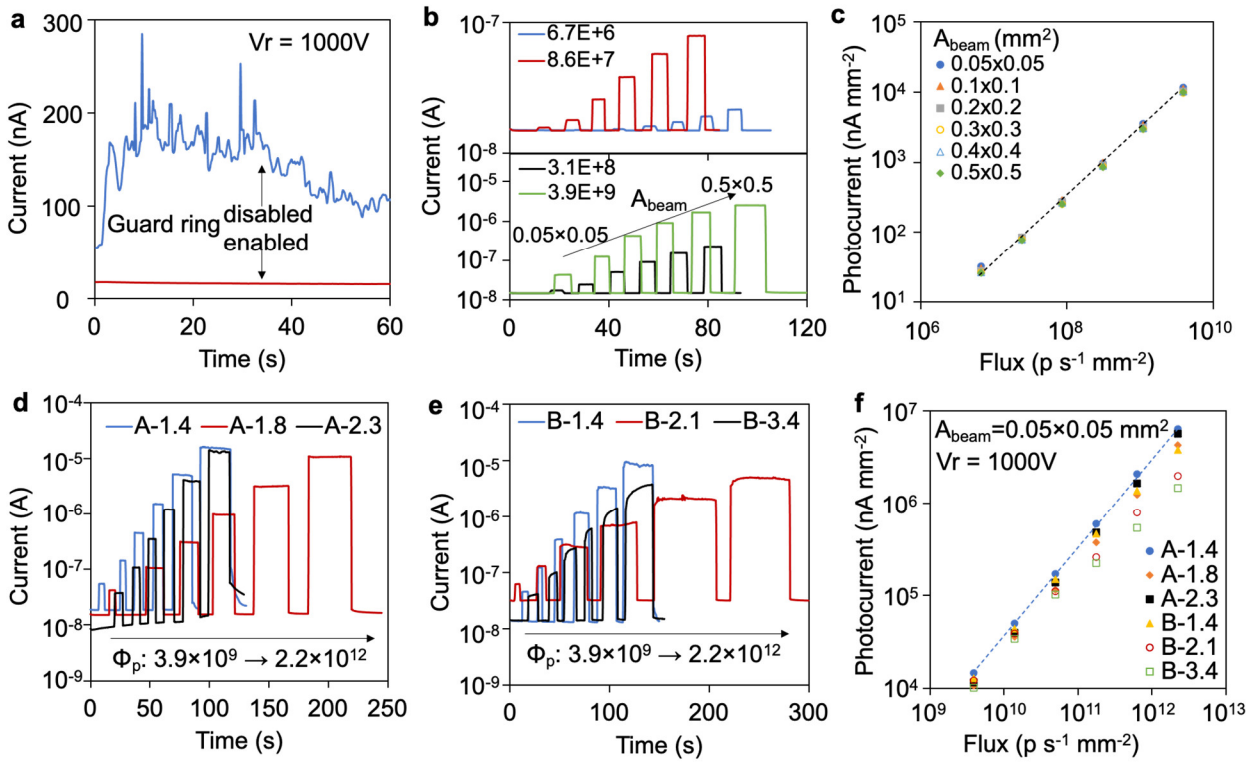

Fig 3. Polarization of $CsPbBr_3$ crystals with different quality. The Au/$CsPbBr_3$/Bi detectors were used for testing. **a,** effect of enable and disabled guard ring electrode in reducing leakage current and increasing reverse bias voltage. **b,** current response as a function of X-ray beam size at different flux values (Vr = 1000 V). **c,** photocurrent against flux at different beam size calculated from data shown in **b**. Data shown in **a, b, c,** were measured from device A-1.8. **d, e,** current response of different devices to X-ray flux in the range $\Phi_p = 3.9\times10^9$ p s^{-1} mm^{-2} to $\Phi_p = 2.2\times10^{12}$ p s^{-1} mm^{-2} (Vr = 1000 V, beam size $A_{beam} = 0.05\times0.05$ mm^2). **f,** photocurrent against flux of different devices calculated from data shown in **d** and **e.**

We have demonstrated that a higher bias voltage could alleviate polarization. However, an overly high bias voltage could cause current instability, deteriorating detector performance. The current instability mainly originates from surface leakage current. Hence, we used a guard ring electrode structure to suppress the surface leakage current, which could further enable an increase in the bias voltage while maintaining a stable dark and signal current. As shown in **Fig 3a**, when the guard ring electrode is disabled (floating), the dark current has large amplitude (~ 100 nA - 200 nA) and fluctuation. On the other hand, enabling the guard ring electrode (by holding it at the same voltage potential as the center electrode) resulted in significantly lower and more stable dark currents (~17 nA) at a bias voltage of 1000 V, which is the upper limit of our instrument. With a high bias voltage of 1000 V, both the dark and signal currents of a $CsPbBr_3$ detector remained stable as the X-ray beam size was varied from 0.05×0.05 mm^2 to 0.5×0.5 mm^2 at a fixed flux (**Fig 3b**). The dark

current during separate tests at different X-ray fluxes stayed unchanged, showing good signal reproducibility of the $CsPbBr_3$ detector. Consequently, good photocurrent linearity as a function of flux was obtained in the flux range of $\Phi_p = 6.7\times10^6$ p s^{-1} mm^{-2} to 3.9×10^9 p s^{-1} mm^{-2} at a bias voltage of 1000 V (556 V mm^{-1}) (**Fig 3c)**. The photocurrent density was consistent across varying beam sizes for the same flux, indicating excellent photocurrent reproducibility. No significant polarization was observed at flux levels up to 3.9×10^9 p s^{-1} mm^{-2}.

Having effectively minimized surface leakage current with the guard ring electrode, we proceeded to investigate the impact of the bulk quality of $CsPbBr_3$ crystals on polarization. We tested the response of the six Au/$CsPbBr_3$/Bi detectors with different crystal quality, as analyzed by photoluminescence measurements in **Fig 1**, under a flux range of $\Phi_p = 3.9\times10^9$ p s^{-1} mm^{-2} to 2.2×10^{12} p s^{-1} mm^{-2}. A bias voltage Vr = 1000 V was used for all devices and the devices were in a fresh non-polarized state before testing. As shown in **Fig 3d**, the signal current of grade A devices showed a small fluctuation and a slight decay at the highest flux of 2.2×10^{12} p s^{-1} mm^{-2}, which indicates radiation-induced polarization. Compared with the grade A devices, device B-1.4 and B-2.1 started to show signal current decay at flux ~ 10^{11} p s^{-1} mm^{-2} (**Fig 3e**), which indicates more prominent polarization than the grade A devices. Besides, device B-3.4 showed a current increasing behavior. Like the current increase of the Bi/$CsPbBr_3$/Bi device at 100 V with flux 3.9×10^9 p s^{-1} mm^{-2} (**Fig 2b**) and at 300V with flux 2.2×10^{12} p s^{-1} mm^{-2} (**Fig 2d**), the slow current increasing of device B-3.4 is due to trap filling. We further compared the photocurrent density as a function of flux for different devices (**Fig 3f**). As the flux increased, the photocurrent deficit against a linear increase gradually became larger for all devices, which is due to more severe polarization at higher flux. At the flux of 2.2×10^{12} p s^{-1} mm^{-2}, all 3 grade B devices had a smaller photocurrent than the grade A devices. Device A-1.4 exhibited the best linearity, attributed to both its high crystal quality and stronger electric field. In contrast, as the crystal quality decreased and the thickness increased, the photocurrent linearity vs flux progressively deteriorated, providing clear evidence that stronger electric fields and higher crystal quality with fewer defects can help mitigate $CsPbBr_3$ polarization.

$CsPbBr_3$ detector trap filling and release behavior

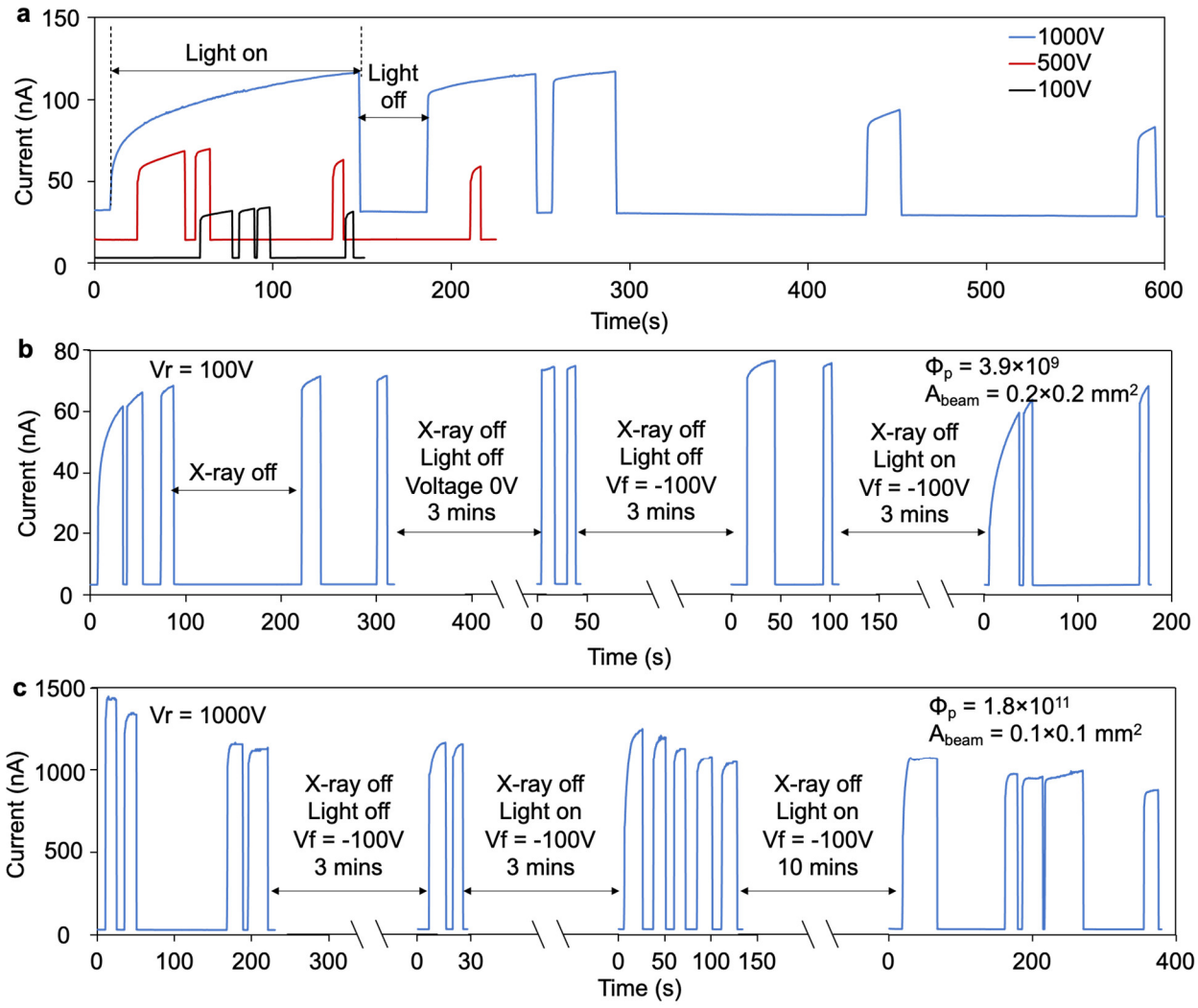

Fig 4. Trap filling and release behavior of $CsPbBr_3$ detector under controlled ambient light, low and high flux X-ray. a, current response to controlled light with "on/off" cycles of different duration. **b,** current response to X-ray flux $\Phi_p = 3.9\times10^9$ p s^{-1} mm^{-2} (Vr = 100 V). Different device treatment was used between "on/off" cycles. **c,** current response to X-ray flux $\Phi_p = 1.8\times10^{11}$ p s^{-1} mm^{-2} (Vr = 1000 V). These data were measured with device B-2.1. Non-polarized respective device area was used for measurement in **b** and **c**. Same respective spot was irradiated during entire measurement of **b** and **c**.

We further studied the $CsPbBr_3$ trap filling and release behavior under light, relatively low and high flux X-rays with the goal to understand how polarization can be suppressed or enhanced. Since the degree of polarization depends on the detector irradiation history, as shown in our previous work[5,6], the detector signal current response was tracked in a series of tests with different treatment methods. The signal current rising and decreasing behavior was then used to deduce the trap filling and release characteristics. We first tested $CsPbBr_3$ detector trap filling and release

behavior under visible light illumination. The current response under a controlled ambient room light (white light with emission covering entire visible light wavelength) with constant intensity was examined. As shown in **Fig 4a**, at a constant bias voltage of 1000 V, when the light was turned on, the $CsPbBr_3$ detector signal current slowly increased in a time scale of more than 100 s, which is due to trap filling as analyzed above for **Fig 2b**. With light off for a period (e.g., tens of seconds), the initial signal current upon turning on the light again became lower than the maximum end current of the preceding cycle of light on, which indicates that a portion of the filled traps were released during the period of light off. Then the initial signal current kept increasing again during the period of light on. The detector current response testing was repeated for several more cycles of light on/off. The amplitude of the initial signal current immediately upon light turned on depends on the duration of the preceding period of light off. The longer the preceding period of light off lasted, the smaller the initial signal current was, suggesting the traps filled by light illumination can empty in dark ambient conditions. The same behavior was also observed at a lower bias voltage of 500 V and 100 V (**Fig 4a**).

We then tested the trap filling and release behavior at a lower flux of $\Phi_p = 3.9\times10^9$ p s^{-1} mm^{-2}. Because trap filling and polarization was negligible at flux of $\Phi_p = 3.9\times10^9$ p s^{-1} mm^{-2} when a high bias voltage of 1000 V was used (as shown in **Fig 3b** and **Fig 3c**), to observe the trap filling behavior, we need to use a low voltage of 100 V where polarization and trap filling was prominent as reflected by the signal current increase. The signal current showed a noticeable increase upon turning on the X-ray (**Fig 4b**). Despite repeated X-ray on/off testing, the signal current remained constant, showing no drop after each period of X-ray being turned off. Instead, each time the X-ray was reactivated, the initial signal current was equivalent to the previous signal current when the X-rays were switched off. The signal current exhibited a continual increase throughout a series of on/off X-ray testing, eventually reaching a saturation point. This suggests that at a low bias voltage of 100 V, the traps filled by X-ray illumination at a flux of 3.9×10^9 p s^{-1} mm^{-2} remain filled and cannot be emptied under dark ambient conditions. This pattern persisted even after the bias voltage was turned off for three minutes and when the voltage direction was reversed from reverse bias Vr = 100 V to forward bias Vf = -100 V for three minutes. However, when the crystal was simultaneously exposed to ambient light and a forward bias Vf = -100 V for three minutes, the signal current saturation was eliminated and the amplitude of the signal current was reversed back to a lower amplitude. The findings indicate that applying a forward bias to the $CsPbBr_3$ detector

while illuminating it with ambient light can release the traps that were filled during low-flux illumination ($\Phi_p = 3.9\times10^9$ p s^{-1} mm^{-2}).

Finally, we tested the $CsPbBr_3$ detector trap filling and release behavior under a relatively high flux of $\Phi_p = 1.8\times10^{11}$ p s^{-1} mm^{-2} where trap filling and polarization is significant even at a high bias voltage of 1000 V (**Fig 4c**). Contrary to the testing under light and low X-ray flux of 3.9×10^9 p s^{-1} mm^{-2}, when the X-ray turned on at high flux of 1.8×10^{11} p s^{-1} mm^{-2}, the initial signal current did not show noticeable increase during the period of X-ray exposure (~ 10 - 20 seconds). During repeated X-ray on/off testing, the signal current gradually decreased because of excessive charge trapping and subsequent polarization. Forward biasing at Vf = -100 V with simultaneous light illumination for 3 mins slightly recovered the increasing behavior and the amplitude of the initial signal current, which implies that only a portion of the filled traps were released. The same behavior was reproduced with light on at Vf = -100 V and treatment time increased to 10 mins. Despite partial trap release, the photocurrent trend was to decrease under the flux of 1.8×10^{11} p s^{-1} mm^{-2}.

The different behavior of $CsPbBr_3$ detector current response under light, low and high flux X-ray suggests trap filling of $CsPbBr_3$ is dependent on the excitation source and flux. Under light illumination, only shallow traps are filled by charge carriers and these traps can be easily released in ambient dark conditions. Under lower X-ray flux of 3.9×10^9 p s^{-1} mm^{-2}, traps with deeper energy level are filled in and these traps can be released by forward biasing with light illumination. In contrast, under higher X-ray flux of 1.8×10^{11} p s^{-1} mm^{-2}, the signal current cannot be recovered by post-polarization treatments, which indicates the filling of very deep traps that cannot be released. These deep traps are probably formed as a result of high flux X-ray irradiation, rather than being pre-existing. If the deep traps were pre-existing, they would still trap charge carriers and cause a decrease in signal current without recovery, even under conditions of light illumination and lower X-ray flux. However, since the photocurrent of the polarized region did not reduce to zero due to the presence of the deep traps, we have concluded that the detector suffered partial in situ damage under the higher X-ray flux (e.g., 1.8×10^{11} p s^{-1} mm^{-2}), rather than complete destruction.

To investigate the energy levels of these newly created deep traps, we performed thermally stimulated current (TSC) measurements. A detailed experiment procedure of the TSC was described in our previous work[29]. Briefly, a $CsPbBr_3$ detector was first photoexcited with a Xe arc

lamp for 15 mins at 79 K to allow trap filling. Then the device was heated up at a constant rate from 79 to 315 K under a constant reverse bias, and the thermally stimulated current was obtained with an electrometer. As shown in **Fig 5**, a polarized $CsPbBr_3$ detector irradiated by X-ray of flux 2.2×10^{12} p s^{-1} mm^{-2} produced a thermally stimulated current that is in the same order (several tens of pA/cm^2) as a fresh non-polarized $CsPbBr_3$ detector. The similar thermally stimulated current magnitude indicates that the polarized region was not electrically active for current contribution during the TSC measurements from 79 K to 315 K. Hence, the energy levels of the deep traps created by ultra-high flux X-ray irradiation may be deeper than 315 K, which exceeds our experimental temperature capability.

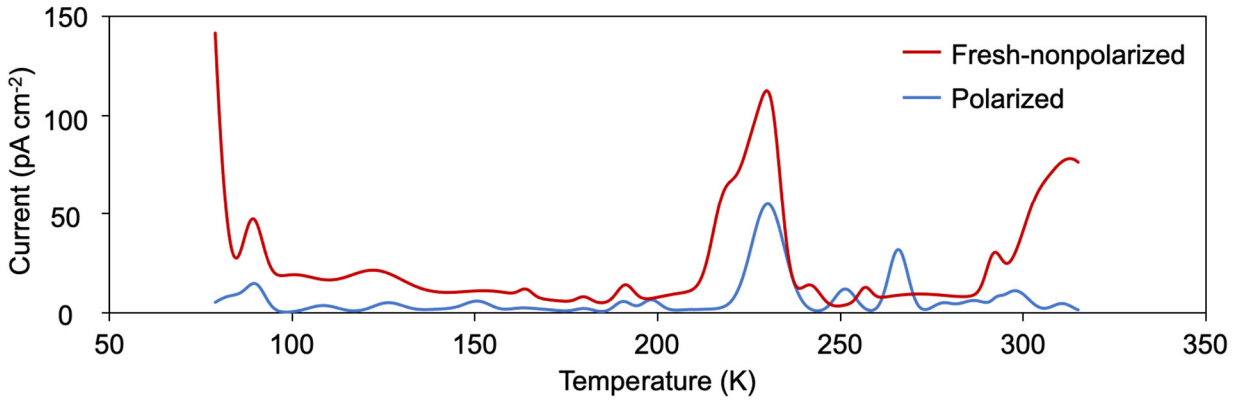

Fig 5. Thermally stimulated current of a fresh nonpolarized and a polarized $CsPbBr_3$ detector in temperature range 79 K – 315 K.

Conclusions

The $CsPbBr_3$ detectors showed good photocurrent linearity and reproducibility at X-ray flux up to 3.9×10^9 p s^{-1} mm^{-2}. In comparison, medical X-rays typically have flux in the range 10^7 – 10^9 p s^{-1} mm^{-2} [1,6]. Hence, the $CsPbBr_3$ detectors are promising for medical X-ray detection. In the flux range 10^{10} - 10^{12} p s^{-1} mm^{-2}, however, the photocurrent linearity in the crystals we tested gradually deteriorated as the X-ray flux increases. $CsPbBr_3$ crystals with more defects had larger photocurrent deficit. Therefore, continued improvements in crystal quality (less defects) and higher bias voltages are expected to be effective in mitigating the radiation-induced polarization of $CsPbBr_3$ detectors and could lead to higher flux tolerances than the ones presented here. Simple post-polarization treatments, such as reversing bias voltage direction and light illumination, could

not effectively de-polarize the $CsPbBr_3$ detector we tested, which indicates a partial detector damage represented by the deep traps created in situ under the ultra-high flux X-ray irradiation. Reducing the number of these deep defects by tuning crystal properties will require enhanced understanding of the structure stability of the material under extremely high X-ray flux conditions.

Acknowledgments

This research was supported in part by the Defense Threat Reduction Agency (DTRA) under the Interaction of Ionizing Radiation with the Matter University Research Alliance (IIRM-URA) under contract number HDTRA1-20-2-0002. This work has proceeded in part of a U.S. Department of Energy Basic Energy Sciences supported collaboration between ANL, SLAC, BNL and Cornell University to explore hi-Z detector materials. The study utilized the resources of the Advanced Photon Source (a U.S. DOE Office of Science user facility operated for the DOE Office of Science by Argonne National Laboratory) under Contract No. DE-AC02-06CH11357. We acknowledge the assistance of Leighanne Gallington, Tiffany Kinnibrugh, Uta Ruett, and Olaf Borkiewicz at the Advanced Photon Source at beamline 11-ID-B. We thank the entire DOE high-Z team at Argonne, Brookhaven, Cornell and SLAC for useful discussions.

Competing interests

Mercouri G. Kanatzidis and Duck Young Chung are cofounders of Actinia Inc, a company that applies perovskite materials to radiation detection.

Data availability

All data are available in the main text.

References

1 Taguchi, K. & Iwanczyk, J. S. Vision 20/20: Single photon counting x-ray detectors in medical imaging. *Med Phys* **40**, 100901 (2013).

2 Pan, L., He, Y., Klepov, V. V., Michael, C. & Kanatzidis, M. G. Perovskite CsPbBr3 single crystal detector for high flux X-ray photon counting. *IEEE Trans on Med Imaging* (2022).
3 Johns, P. M. & Nino, J. C. Room temperature semiconductor detectors for nuclear security. *J Appl Phys* **126**, 040902 (2019).
4 Veale, M. C. *et al.* Cadmium zinc telluride pixel detectors for high-intensity x-ray imaging at free electron lasers. *J Phys D: Appl Phys* **52**, 085106 (2018).
5 Pan, L. *et al.* Perovskite CsPbBr3 single-crystal detector operating at 1010 photons/s/mm2 for ultra-high flux X-ray detection. *Adv. Optical Mater*. 2202946. (2023).
6 Strassburg, M., Schroeter, C. & Hackenschmied, P. CdTe/CZT under high flux irradiation. *Journal of instrumentation* **6**, C01055-C01055 (2011).
7 Bale, D. S. & Szeles, C. Nature of polarization in wide-bandgap semiconductor detectors under high-flux irradiation: Application to semi-insulatingCd1−xZnxTe. *Physical review. B, Condensed matter and materials physics* **77** (2008).
8 Gadkari, D. *et al.* Characterization of 128× 128 MM-PAD-2.1 ASIC: a fast framing hard x-ray detector with high dynamic range. *Journal of Instrumentation* **17**, P03003 (2022).
9 Baussens, O. *et al.* Characterization of High-Flux CdZnTe with optimized electrodes for 4th generation synchrotrons. *Journal of Instrumentation* **17**, C11008 (2022).
10 Kozlov, V., Kemell, M., Vehkamäki, M. & Leskelä, M. Degradation effects in TlBr single crystals under prolonged bias voltage. *NIMA* **576**, 10-14 (2007).
11 Vaitkus, J. *et al.* Investigation of degradation of electrical and photoelectrical properties in TlBr crystals. *NIMA* **531**, 192-196 (2004).
12 Cola, A. & Farella, I. The polarization mechanism in CdTe Schottky detectors. *Appl Phys Lett* **94** (2009).
13 Datta, A., Fiala, J., Becla, P. & Motakef, S. Stable room-temperature thallium bromide semiconductor radiation detectors. *APL Materials* **5**, 106109 (2017).
14 Takagi, K. *et al.* Bias Polarity Switching-Type TlBr X-Ray Imager. *IEEE Trans on Nuclear Science* **68**, 2435-2439 (2021).
15 Dědič, V. *et al.* De-polarization of a CdZnTe radiation detector by pulsed infrared light. *Appl Phys Lett* **107**, 032105 (2015).
16 He, Y., Hadar, I. & Kanatzidis, M. G. Detecting ionizing radiation using halide perovskite semiconductors processed through solution and alternative methods. *Nature photonics* (2021).
17 Tsai, H. *et al.* Quasi-2D Perovskite Crystalline Layers for Printable Direct Conversion X-Ray Imaging. *Advanced Materials* **34**, 2106498 (2022).
18 Pan, L., Feng, Y., Kandlakunta, P., Huang, J. & Cao, L. R. Performance of Perovskite CsPbBr3 Single Crystal Detector for Gamma-Ray Detection. *IEEE trans on nucl sci* **67**, 443-449 (2020).
19 He, Y. *et al.* High spectral resolution of gamma-rays at room temperature by perovskite CsPbBr3 single crystals. *Nat Commun* **9**, 1609 (2018).
20 He, Y. *et al.* Sensitivity and Detection Limit of Spectroscopic-Grade Perovskite CsPbBr3 Crystal for Hard X-Ray Detection. *Advanced Functional Materials*, 2112925 (2022).
21 Prokesch, M., Soldner, S. A. & Sundaram, A. G. CdZnTe detectors for gamma spectroscopy and x-ray photon counting at 250 × 106 photons/(mm2 s). *J Appl Phys* **124**, 44503 (2018).

22 Sedigh Rahimabadi, P., Khodaei, M. & Koswattage, K. R. Review on applications of synchrotron-based X-ray techniques in materials characterization. *X-Ray Spectrometry* **49**, 348-373 (2020).
23 Tang, F. *et al.* Synchrotron X-Ray Tomography for Rechargeable Battery Research: Fundamentals, Setups and Applications. *Small Methods* **5**, 2100557 (2021).
24 Westneat, M. W., Socha, J. J. & Lee, W.-K. Advances in biological structure, function, and physiology using synchrotron X-ray imaging. *Annual Review of Physiology* **70**, 119-142 (2008).
25 Pan, L., Feng, Y., Huang, J. & Cao, L. R. Comparison of Zr, Bi, Ti, and Ga as Metal Contacts in Inorganic Perovskite $CsPbBr_3$ Gamma-Ray Detector. *IEEE transactions on nuclear science* **67**, 2255-2262 (2020).
26 He, Z. Review of the Shockley–Ramo theorem and its application in semiconductor gamma-ray detectors. *NIMA* **463**, 250-267 (2001).
27 Jia, P. *et al.* The Trapped Charges at Grain Boundaries in Perovskite Solar Cells. *Advanced Functional Materials* **31**, 2107125 (2021).
28 Zeng, P., Feng, G., Cui, X. & Liu, M. Revealing the role of interfaces in photocarrier dynamics of perovskite films by alternating front/back side excitation time-resolved photoluminescence. *The Journal of Physical Chemistry C* **124**, 6290-6296 (2020).
29 Peters, J. A., Liu, Z., De Siena, M. C., Kanatzidis, M. G. & Wessels, B. W. Defect levels in CsPbCl3 single crystals determined by thermally stimulated current spectroscopy. *J Appl Phys* **132**, 035101 (2022).